Descending Staircase in the UGent Knee Rig: a Feasibility Study

Amélie Chevalier [*] **Jan Victor** [**] **Stijn Herregodts** [*,**]
Mia Loccufier [*]

[*] *Department of Electromechanical, Systems and Metals Engineering, Ghent University, Belgium, (e-mail: amelie.chevalier@ugent.be)*
[**] *Department of Human Structure and Repair, Ghent University Hospital, Belgium*

Abstract: The objective of this work consists of studying the feasibility to impose descending stair negotiation in the UGent Knee Rig (UGKR). The force and position reference signals for the control strategy are derived from literature. A mathematical coordinate transformation is developed to make the stair descent possible within the limitations of the UGKR. Kinematic measurements of the six degrees of freedom in the knee joint allow to assess knee instability. Therefore, a kinematic measurement method based on CT-images is used to measure the relative position of the bones during the stair descent. First, the study is performed on a mechanical knee hinge to evaluate the performance of the position and force control. Second, a saw-bone study is performed to assess the kinematic measurement. The results show the feasibility of the developed method to impose stair descent motions in future cadaver studies.

Keywords: Descending stair, Knee Kinematics, Dynamic kee rig, Biomedical Control, Joint trajectory

1. INTRODUCTION

Total knee replacement (TKR) is the procedure where a knee implant is inserted in patients. However, literature study shows that 10% of the patients are dissatisfied afterwards Choi and Ra (2016). It is shown that instability is the second major reason for implant failure Sharkey et al. (2014). This instability has a big influence on patient satisfaction as shown by Van Onsem et al. (2020). Patients suffering from instability after TKR typically complain about problems when descending stairs Schwab et al. (2005).

In-vitro studies in dynamic knee rigs are performed to investigate new implant designs and surgical techniques Arnout et al. (2020). The UGent Knee Rig (UGKR) is a dynamical knee rig which is able to impose squat and bicycle motions onto cadaver specimens Chevalier et al. (2017). Traditional knee rigs used in in-vitro studies are able to impose squats and lunges Maletsky and Hillberry (2005), however, imposing descending staircase motions is missing in literature. To the authors knowledge, only one study attempted in-vitro descending staircase studies Borque et al. (2015). However, due to the limitation in their activity simulator, Borque et al. (2015) could only simulate static phases of the stair descent.

Different stair negotiation methods are presented in literature. A traditional step-over-step is used in normal movements. Older and disabled persons often opt for a step-by-step negotiation or sideways motions (Reid et al. (2007); King et al. (2018)). The end-goal of this ongoing project is the comparison of in-vivo and in-vitro post-operative patients after total knee replacement. This yields the choice of simulating step-over-step stair negotiation in the UGKR.

A literature study of stair negotiation is performed with a focus on reported knee and hip flexion angles and quadriceps and hamstring forces during stair descent using the step-over-step method. Bulea et al. (2014) report on joint angles for a step-by-step method and the accompanying activation of the muscles. For the muscle force of the hamstrings and quadriceps during stair descent, Navacchia et al. (2017) report the hamstring force and quadriceps force during stair descent. The quadriceps force during stair descent in osteoarthritis patients is reported in Fok et al. (2013). Recently, McClelland et al. (2014) have investigated patterns in the knee flexion-extension moments during stair descent in patients after TKR.

From literature different phases in step-over-step stair negotiation are defined Bulea et al. (2014); Navacchia et al. (2017). The stair cycle starts with the heel strike at 0% of stair cycle which is the start of the stance phase. At 20% of the stair cycle, the controlled lowering starts. At 33.3% the hip is in the position above the standing leg. At 50% the contralateral heelstrike takes place. The toe off phase is at 61% of the stair cycle and starts the swing phase. At 83% the hip moves above the contralateral leg. These phases will be used throughout the paper to interpret the results.

This paper is structured as follows. Section 2 presents the methods used to define the position references and force references. This will allow for full simulation of the stair cycle which is a novelty to the state of art. Also the kinematic measurement algorithms are presented. Section

3 presents the results for the mechanical knee hinge and the sawbone stair negotiation in the UGKR followed by a conclusion section.

2. METHODS

A detailed description of the UGent Knee Rig (UGKR) and its control architecture can be found in Chevalier et al. (2017). The control strategy consists of decoupled PID control with feedforward action and gain adaptation. The UGKR controls the ankle position in the sagittal plane. This requires a horizontal ankle profile and a vertical ankle profile. The forces controlled in the UGKR are the quadriceps force and the hamstring force. For the latter, the total hamstring force is split in a medial and lateral component symmetrically. In this study, the specimens inserted in the UGKR are a mechanical knee hinge to ascertain the control of the forces and positions and a sawbone model to measure the knee joint kinematics (Fig.1).

2.1 References for position

The measured flexion angles in hip and knee reported in Bulea et al. (2014) are used to distill the ankle position in the sagittal plane during stair descent. The joint angles are combined with femur and tibia lengths of the knee specimen to calculate the ankle trajectory using cosine-rules. This profile is shown in Fig. 2. Here some assumptions are made:

- The height of the stair steps is 17 cm and the width of the stair steps is 30 cm. This corresponds to values reported in literature Standifird et al. (2014). These measurements are the same as the stair which is used during on-going in-vivo fluoroscopy studies in post-operative patients in our department.
- The center of the hip joint descends linearly according to the steepness of the stairs.
- The movement from where the foot is in full contact until toe off phase (= heel rise phase) is a rotation around the center of the metatarsophalangeal joints.
- The maximal extension of the specimen corresponds with a flexion angle of 20°. This is to keep the specimen intact during measurements.

As the hip joint in the UGKR is fixed in space, this profile is impossible to implement in the setup. By using coordinate transformations, this problem is mitigated. The result of this coordinate transformation is an experiment where

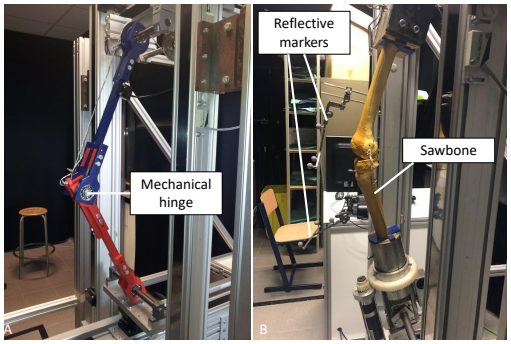

Fig. 1. Mechanical knee hinge and sawbone specimen.

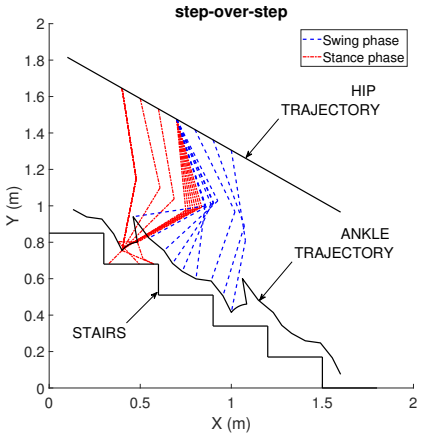

Fig. 2. Stair profile based on literature.

a person is descending an escalator while it is moving upwards. If the descending speed of the person matches the speed of the moving escalator, this creates the illusion of a fixed hip joint while the person is still performing the motion of a stair descent. The coordinate transformation used in this research consists of two steps: 1) a translation and 2) a trajectory following. The translation places the coordinate system (X, Y) in the hip joint at (H_X, H_Y) which is the physical coordinate of the hip joint in the rig. Afterwards, the trajectory of the hip (h_x, h_y) in the sagittal plane is followed by the coordinate system. The total coordinate transformation can be expressed using the following equation:

$$a_{x'} = a_x - h_x + H_X \quad (1)$$

$$a_{y'} = a_y - h_y + H_Y \quad (2)$$

where (a_x, a_y) is the ankle trajectory in coordinate system (X, Y) and $(a_{x'}, a_{y'})$ is the ankle trajectory in the moving coordinate system (X', Y').

The resulting ankle profile in the moving coordinate system (X', Y') is a cyclic motion in the sagittal plane (Fig. 3a). Note that the physiological path of the ankle, does not contain discontinuities. Therefore, the profile based on discrete literature measurements (sampled data), is smoothed using shape prescriptive curve fitting. This is a technique which uses least squares splines subject to simple constraints. The constraints allow for a physiological profile where the ankle is fixed in space during the stance phase. This allows for a clear distinction in the phases of the stair negotiation, which would be compromised when using unconstrained splines due to fitting errors. The resulting smooth ankle trajectories in function of time are shown in Fig. 3b. Here, the vertical lines indicate the different phases reported in literature (1=heel strike, 2=controlled lowering, 3=hip above standing leg, 4=contralateral heelstrike, 5=toe off, 6=hip above contralateral leg, 7=heelstrike).

Note in Fig. 3b, the total time of one step is 25 s. The reason is twofold: 1) To keep the cadaver specimen intact during measurements, it is advised to lower the speed, 2) To meet the physical limitations of the position actuators. The maximal speed for the horizontal and vertical actuator is 174 mm/s and 122 mm/s respectively. Fig. 4 shows the calculated speed of the horizontal and vertical actuator. Literature reports a stair descent velocity of 0.76 m/s Fok

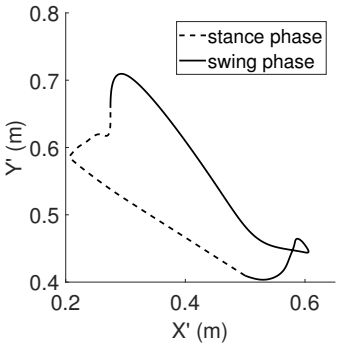

(a) Ankle position in sagittal plane after coordinate transformation and smoothing.

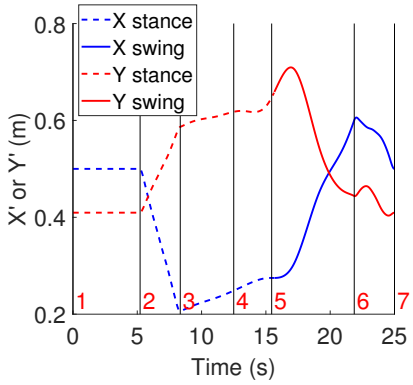

(b) Horizontal and vertical ankle position in the sagittal plane in function of time.

Fig. 3. Ankle trajectories.

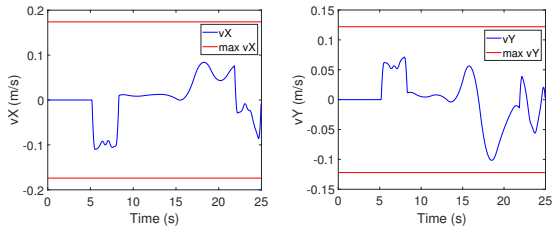

Fig. 4. Speed of the position actuators.

et al. (2013). Combining this velocity with a stair width of 30 cm and a stair height of 17 cm Standifird et al. (2014), yields a gait speed of approximately 1 s. However, this physiological speed far exceeds the limitations of the actuator and is not realistic in the context of cadaver studies. An iterative process shows that simulating a gait cycle of 25 s, yields satisfactory motor speeds.

The resulting profile can be adjusted for each cadaver specimen by performing a calibration before the test where the Y-position of the ankle is measured for the maximal flexion angle. This Y-position is then set a starting point of the vertical profile of the ankle.

2.2 References for forces

The second step is creating reference profiles for the applied quadriceps and hamstring force. The reported force profiles of Navacchia et al. (2017); Fok et al. (2013) are combined in a quadriceps and hamstring profiles shown in Fig. 5. Note here that the same gait cycle is applied as in the previous section and the same curve fitting techniques is applied on the sampled data. A reduction with factor 2.5 is used on the forces reported in literature to keep the specimen intact as reported in Dockers and Stevens (2006). Here, it is shown that the integrity of the cadaver ligaments is compromised, yielding the need for lower applied forces. In Fig. 5, the different phases in the stair cycles are also indicated.

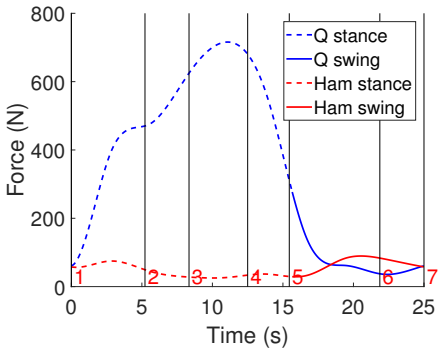

Fig. 5. Quadriceps force (Q) and hamstring force (Ham) profiles based on literature.

2.3 Kinematic measurements

To evaluate the kinematics of the knee joint during the stair descent, a CT-based monitoring system is used. Fig. 6 shows a flowchart of the kinematic measurement procedure.

From the CT-images an STL mesh of the femur and tibia is segmented. Reflective markers are attached to the femur and tibia while being tracked with an infrared camera system (OptiTrack, NaturalPoint, Corvallis, Oregon, USA). During a registration step (no movement), the surface of the bone is captured as a point cloud using reflective markers and an Iterative Closest Point (ICP) algorithm is used to define the needed transformation matrix to transform the STL mesh in the camera coordinate system. Also the position of the fixed bone markerset is captured and combined with the coordinates of bony landmarks from CT to define a body-fixed coordinate system for each bone. For the femur, this coordinate system is defined by the hip center and femoral intercondylar notch (mechanical axis) and the medial and lateral flexion facet centers (medio-lateral axis). For the tibia, this body-fixed coordinate system is defined by the ankle center and tibial spine (mechanical axis) and the centers of the medial and lateral tibial plateau (medio-lateral axis).

After registration, the specimen is subjected to motion and the position of the bone markerset is captured for each frame of the cameras. What follows is a series of algorithms to calculate the needed transformation matrices to bring the STL mesh of the bone in the camera coordinate system. The result is the movement of the bones in the UGKR. Afterwards, a back transformation algorithm is used to bring the bones back into the stairs.

The kinematics are described in line with the original work of Grood and Suntay (1983) resulting in translations of the knee joint in three directions (medio-lateral, anteroposterior and distraction-compression) and three

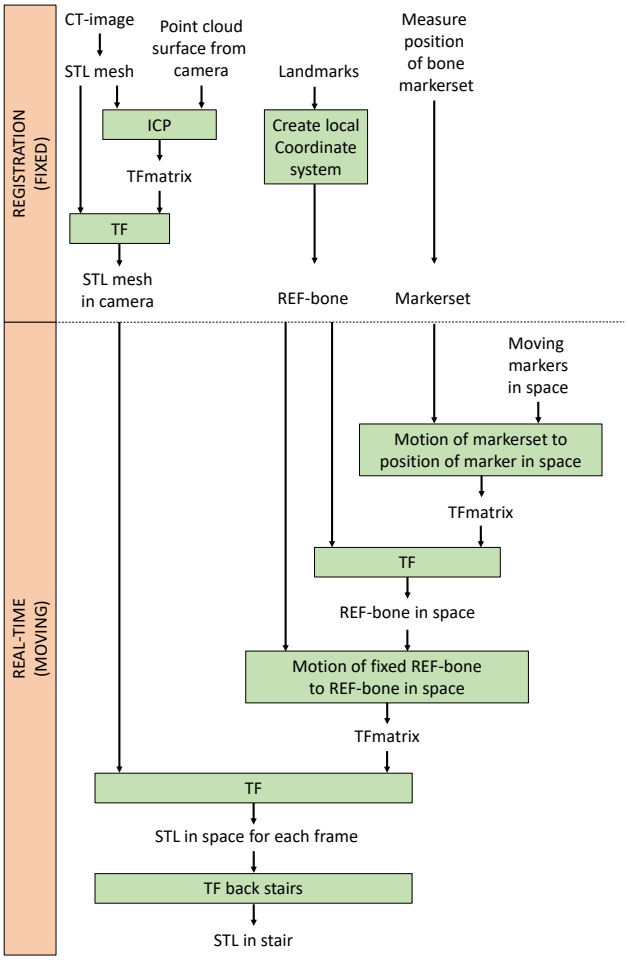

Fig. 6. Flowchart of the kinematic measurement procedure where TF stands for transformation matrix.

rotations (flexion-extension, varus-valgus and internal-external). From both body-fixed coordinate systems, a joint coordinate system with a floating anteroposterior axis is subsequently derived to describe the joint kinematics in six degrees of freedom.

3. RESULTS

3.1 Mechanical knee hinge

The position and force control strategy with the newly developed reference signals is tested on a mechanical knee hinge (Fig. 1a). A series of 10 stair steps are measured in the UGKR to show the repeatability of the system (Fig. 7). It is clear from Fig. 7 that each step can be done with a high level of repeatability. The average maximal error on the X-position, Y-position, quadriceps forces and hamstring force are 3.22 mm, 2.48 mm, 46.04 N and 17.87 N respectively which is comparable to literature Forlani et al. (2016). Note here that the maximal error on the quadriceps force takes place only in a short time after phase 2 which is the start of the controlled lowering. At this point there is a sudden start of movement, inducing a larger error for a short time (0.21 s). Excluding this peak, the maximal error on the quadriceps force in 20.21 N.

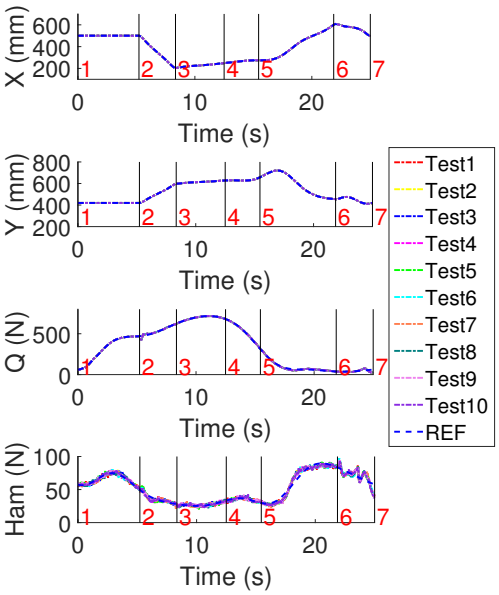

Fig. 7. Measured position and forces in the UGKR for the mechanical knee hinge.

3.2 Sawbones

After testing the function of the force and position trajectory following, the kinematic measurement feasibility study is performed by inserting a sawbone model of the knee joint (Fig. 1b). Sawbones are made of solid foam and give a replica of the bone surface needed for the kinematic measurements. However, the solid foam does not have the mechanical properties of real bone, thus limiting the possibility of applying the quadriceps and hamstring forces. Therefore, three kinematic stair cycles were measured by applying only the ankle position references.

Control performance The resulting trajectory following for the ankle position is shown in Fig. 8. The average maximal error on the X-position and Y-position are 3.17 mm and 2.40 mm respectively.

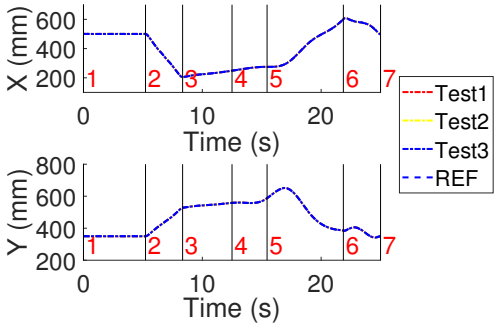

Fig. 8. Measured position in the UGKR for the sawbones.

Kinematic tracking During the registration step, the surface of the bone is registered and matched to the segmented STL file from the CT images, using the ICP algorithm. The result can be seen for the tibia in Fig. 9. The matching rms error from the ICP algorithm is

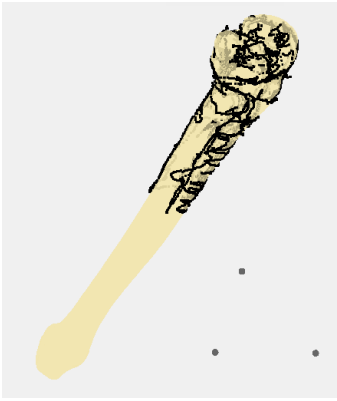

Fig. 9. Point cloud registration of the surface of the tibia.

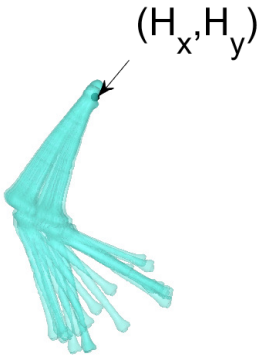

Fig. 10. Bones in the UGKR.

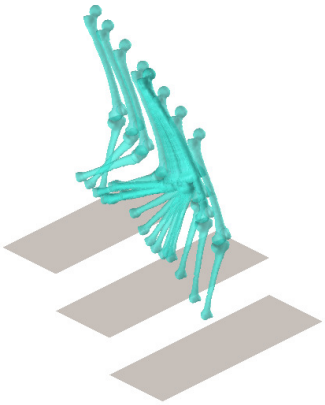

Fig. 11. Bones during stair descent.

0.96 mm for the tibia. Similar results are obtained for the registration of the femur.

Afterwards the real-time kinematic tracing is done for the descending stair. The resulting positions of the femur and tibia in the UGKR are shown in Fig. 10. Here, the anatomical position of the hip is indicated by (H_X, H_Y).

After obtaining the bone positions in the UGKR coordinate system, the backwards transformation is performed to obtain the position of the bones during the stair cycle. This is shown in Fig. 11.

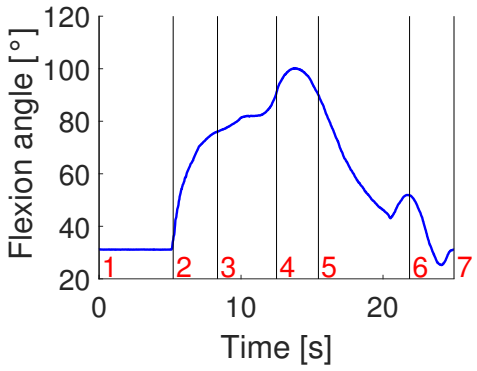

Fig. 12. Measured flexion angle

The kinematics are expressed as three translations and three rotations. The angles and displacements expressed here are the displacement and rotation of the femur with respect to the fixed tibia. All displacements and rotations are expressed in function of the flexion angle shown in Fig. 12 according to biomechanical convention. The kinematic results are shown in Fig.13. These results show the kinematic measurements averaged over the three measured stair cycles. The three translations are here expressed for the medial and lateral compartment of the knee joint.

This study has some limitations. In this work, a reference signal for stair descent is designed to obtain a physiological stair descent motion. To the authors knowledge, this is the most optimal signal taken into account the dimensions of the stair provided and the actuator speed limitations. A second limitation is the work on sawbones. No comparison of the kinematic parameters can be done as no sawbone data is published. Future work on cadaver specimens will mitigate this limitation and allow for comparison with literature such as Borque et al. (2015).

4. CONCLUSION

This work presents a feasibility study on performing descending staircase motions in the UGent Knee Rig (UGKR). Studying descending staircase in-vitro on cadaver specimens is of vital importance for instability studies in post-operative patients after total knee replacement. The study shows that the UGKR is capable of imposing the required motions and force profiles to perform the stair descent. Kinematic measurements based on CT images, allow to visualize the bones during the motion. The developed coordinate transformations allow to transform the motions in the UGKR back to the stair motion. Future work is a series of cadaver studies to investigate knee instability during stair descent in native and post-operative situations with the final goal to increase patients satisfaction after total knee replacement.

ACKNOWLEDGEMENTS

The authors acknowledge the work of Thibeau Vancouillie, Bert De Coninck and Matthias Verstraete for their work for the kinematic algorithms.

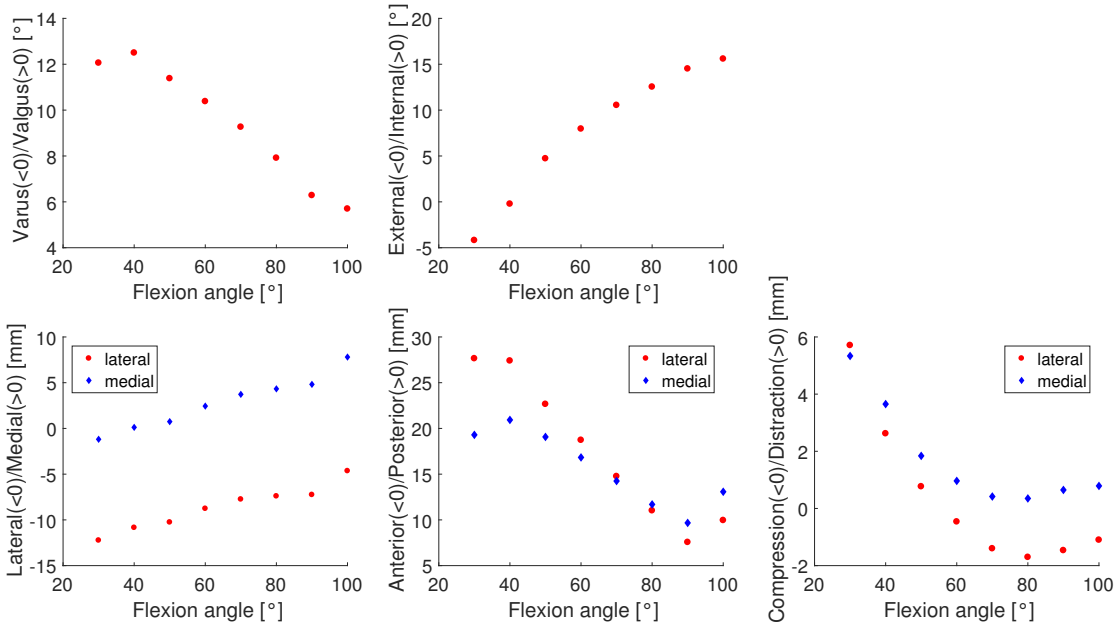

Fig. 13. Measured knee joint kinematics during stair descent.

REFERENCES

Arnout, N., Victor, J., Chevalier, A., Bellemans, J., and Verstraete, M. (2020). Muscle loaded stability reflects ligament-based stability in tka : a cadaveric study. *Knee Surgery Sports Traumatology Arthroscopy*, doi:10.1007/s00167-020-06329-2.

Borque, K.A., Gold, J.E., Incavo, S.J., Patel, R.M., Ismaily, S.E., and Noble, P.C. (2015). Anteroposterior knee stability during stair descent. *The Journal of Arthroplasty*, 30, 1068–1072.

Bulea, T.C., Kobetic, R., Audu, M., Schnellenberger, J.R., Pinault, G., and Triolo, R. (2014). Forward stair descent with hybrid neuroprosthesis after paralysis: Single case study demonstrating feasibility. *Journal of Rehabilitation Research & Development*, 51, 1077–1094.

Chevalier, A., Verstraete, M., Ionescu, C., and Keyser, R.D. (2017). Decoupled control for the bicycling ugent knee rig: Design, implementation, and validation. *IEEE/ASME Transactions on Mechatronics*, 22, 1685–1694.

Choi, Y. and Ra, H. (2016). Patient satisfaction after total knee arthroplasty. *Knee Surg Relat Res*, 28, 1–15.

Dockers, K. and Stevens, V. (2006). *Research into the forces of the patellofemoral joint and the design and construction of an experimental load model*. Master's thesis, Ghent University.

Fok, L., Schache, A., Crossley, K., Lin, Y., and Pandy, M. (2013). Patellofemoral joint loading during stair ambulation in people with patellofemoral osteoarthritis. *Arthritis Rheum*, 65, 2059–2069.

Forlani, M., Sancisi, N., Conconi, M., and Parenti-Castelli, V. (2016). A new test rig for static and dynamic evaluation of knee motion based on a cable-driven parallel manipulator loading system. *Meccanica*, 51, 1571–1581.

Grood, E. and Suntay, W. (1983). A joint coordinate system for the clinical description of three-dimensional motions: Application to the knee. *Journal of Biomechanical Engineering*, 105, 136–144.

King, S., Underdown, T., Reeves, N., Baltzpopoulos, V., and Maganaris, C. (2018). Alternate stair descent strategies for reducing joint moment demands in older individuals. *Journal of Biomechanics*, 78, 126–133.

Maletsky, L. and Hillberry, B. (2005). Simulating dynamic activities using a five-axis knee simulator. *Journal of Biomechanical Engineering*, 127, 123–133.

McClelland, J., Feller, J., Menz, H., and Webster, K. (2014). Patterns in the knee flexion-extension moment profile during stair ascent and descent in patients with total knee arthroplasty. *J Biomech*, 47, 1816–1821.

Navacchia, A., Rullkoetter, P., Schütz, P., R. List, C.F., and Shelburne, K. (2017). Subject-specific modelling of muscle forces and knee contact in total knee arthroplasty. *Journal of Orthopaedic Research*, 34, 1576–1587.

Reid, S., Lynn, S., Musselman, R., and Costigan, P. (2007). Knee biomechanics of alternate stair ambulation patterns. *Medicine & Science in sports & exercise*, 39, 2005–2011.

Schwab, J., Haidukewych, J., Hanssen, A., Jacofsky, D., and Pagnano, M. (2005). Flexion instability without dislocation after posterior stabilized total knees. *Clin Orthop Relat Res*, 440, 96–100.

Sharkey, P., Lichstein, P., Shen, C., Tokarski, A., and Parvizi, J. (2014). Why are total knee arthroplasties failing today?–has anything changed after 10 years? *J Arthroplasty*, 29, 1774–1778.

Standifird, T., Cates, H., and Zhang, S. (2014). Stair ambulation biomechanics following total knee arthroplasty: a systematic review. *The Journal of Arthroplasty*, 29, 1857–1862.

Van Onsem, S., Verstraete, M., Van Eenoo, W., Van Der Straeten, C., and Victor, J. (2020). Are tka kinematics during closed kinetic chain exercises associated with patient-reported outcomes? a preliminary analysis. *Clin Orthop Relat Res*, 478, 255–263.